Journal of Solid State Chemistry **168,** 486–496 (2002)
doi:10.1006/jssc.2002.9733

Peculiarity of Hexamethylenetetratellurafulvalene (HMTTeF) Charge Transfer Complexes of Donor–Acceptor (D–A) Type

Sang-Soo Pac[1] and Gunzi Saito

Division of Chemistry, Graduate School of Science, Kyoto University, Sakyo-ku, Kyoto 606-8502, Japan

Received December 18, 2001; in revised form May 5, 2002; accepted May 17, 2002

The complex formation of hexamethylenetetratellurafulvalene (HMTTeF) with 28 kinds of organic electron acceptors yielded 31 charge transfer (CT) complexes. The infrared and ultraviolet–visible–near-infrared spectra of the complexes were examined to study the ionicity of their ground states in solid. A plot of CT transition energies and the difference of redox potentials; ΔE(DA) of donor (D) and acceptor (A) molecules indicated that four complexes have a neutral ground state. Four other complexes exhibit characteristic features of a fully ionic ground state based on the vibrational spectra. Notably, the HCBD, F_4TCNQ and DDQ complexes indicate both a relatively low first CT band and high conductivity in a solid in spite of the fully ionic character being very plausible. Twenty-three complexes having a partially ionic ground state have a CT band below $4 \times 10\,cm^{-1}$ and are highly conductive. The preparation of good single crystals of the HMTTeF complexes for structural analysis was only successful with Et_2TCNQ and BTDA-TCNQ, which have the structure of DA alternately stacking. These two complexes indicate high conductivities in spite of their disadvantageous packing manner. The intermolecular interactions are found to be strongly enhanced by both the bulky molecular orbital of HMTTeF and the decreased on-site Coulomb repulsion in the HMTTeF complexes. These two factors in particular seem to prevent both the fully ionic and the DA alternating HMTTeF complexes from becoming insulators, even though the redox parameters and the crystal structures predict them to be insulating. © 2002 Elsevier Science (USA)

Key Words: **tellurium; HMTTeF; charge transfer complex; conductivity; IR spectrum; UV–Vis–Nir spectrum; donor; acceptor; F_4TCNQ.**

INTRODUCTION

Among the large number of recent studies on the organic metals and superconductors of charge transfer (CT) complexes, tellurium-containing (1) donors have been attracting considerable interest for their usefulness to yield highly conductive materials. It has been suggested that using tellurium analogues instead of thia- or selenafulvalenes as electron donors has great advantages with respect to increasing the polarizability, conduction bandwidth, and intermolecular interaction, and also decreasing on-site Coulomb repulsion due to both the large van der Waals radius and small atomic electronegativity of the tellurium atoms (2). These features, alone or in combination, may make the organic CT complexes highly conductive and suppress the metal–insulator (Peierls) transition which inevitably accompanies the low-dimensional nature of these compounds (3). Suppression of the Peierls transition in low-dimensional organic metals is a fundamental requirement to obtain an organic superconductor, therefore, it is worth investigating the chemical and physical properties of tellurium donors and their complexes to synthesize exotic organic metals and superconductors.

Hexamethylenetetratellurafulvalene (HMTTeF) (Scheme 1), which was first synthesized by Wudl and Aharon-Sharom (4), is one of the most available tellurium-containing donor molecules. Some CT complexes of HMTTeF have been prepared with organic acceptors as donor (D)–acceptor (A)-type complexes, and counter anions as cation radical salts (1,5,6). However, the nature of HMTTeF and its CT complexes is not sufficiently understood yet.

The electric conductivities of the CT complexes of HMTTeF with TCNQs (for this and other chemical abbreviations in text, see Ref (7), *p*-quinones, and other π-acceptors (D–A type complexes) have been measured on compaction samples in the previous paper and several highly conductive complexes have been found among them (1). We also previously studied two kinds of metals (1 : 1 TCNQ and Me_2TCNQ complexes) (6). Here we describe the preparation of 31 D–A-type complexes of HMTTeF and give the electronic spectra for each to elucidate the correlation between their electronic and electric states. We

[1]To whom Correspondence should be addressed. pac@kuchem.kyoto-u.ac.jp, saito@kuchem.kyoto-u.ac.

0022-4596/02 $35.00

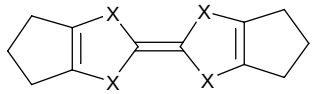

X=S: HMTTF
X=Se: HMTSF
X=Te: HMTTeF

SCHEME 1. HMTTF, HMTSF and HMTTeF

also give evidence that the tellurium donor contributes extraordinarily to the electric conduction compared to sulfur and selenium donors.

EXPERIMENTAL

General

Cyclic voltammetric measurements were performed in 0.1 M solutions of $(TBA)BF_4$ in AN or DCE with Pt working and counter electrodes vs saturated calomel electrode (SCE) at a scan speed of 10–20 mVs^{-1} using a Yanaco Polarographic Analyzer P-1100 at 20–22°C. Optical measurements were made for both in a KBr pellet on a Perkin-Elmer 1600 Series FT-IR (resolution 4 cm^{-1}) for the infared (IR) and near-IR (NIR) regions (400–7800 cm^{-1}) and on a SHIMADZU UV-3100 spectrometer for the ultra-violet–visible–NIR UV–Vis–NIR region (3800–42000 cm^{-1}). Electronic absorption spectra were also measured in DCE solution. Crystal densities were determined using the floating method with a mixture of 1,2-dibromoethane and diiodemethane. DC conductivities were measured by either a standard two- or four-probe technique, using gold paste (Tokuriki No.8560-1A) to attach gold wires to the samples. For powdered samples, measurements were performed on compressed pellets which were cut to form an orthorhombic shape.

Preparation of HMTTeF Complexes

HMTTeF was synthesized according to the reported procedure by Wudl and Aharon-Sharom (4), and purified by repeated recrystallization. The isomer, tetratelluradicyclopenta[b,g]naphthalene (TTeDCN) (8) was separated under a microscope. DDQ, TCNQ, TCNE, QCl_4, $QBr_2(OH)_2$, $QCl_2(OH)_2$, *s*-TNB and C_{60} were purchased. The following organic acceptors and electrolytes were synthesized in our laboratory according to the literatures: HCBD (9e), F_4TCNQ (9b), DBDQ (9c), DIDQ (9d), CF_3TCNQ (9b,e,f), F_2TCNQ (9b,e,f), DCNNQ (9 g), FTCNQ (9b,e,f), DTENF (9 h), DCNQ (9i), MeTCNQ (9b,e,f), Et_2TCNQ (9f), Me_2TCNQ (9f), TCNNQ (9e), $(MeO)_2$TCNQ (9f),BTDA-TCNQ (9j), DTNF (9k), $(EtO)_2$TCNQ (9b,e,f) and H_2TNBP (9 l). All these acceptors were purified by repeated recrystallization, sublimation and/or gradient sublimation on Teflon and identified by melting point and IR spectra. Elemental analysis was also utilized for identification of the materials synthesized. DHBTCNQ and THBTCNQ were kindly supplied by Prof. K. Nakasuji. Scheme 2 shows the chemical structures of the 28 organic acceptors and anions used in this work.

D–A type complexes were usually prepared by mixing two hot solutions of each component in PhCl, DCE, THF, toluene or a mixture of those solvents with about 1 : 1 of D : A molar ratio. Single crystals of the Me_2TCNQ complex were obtained by diffusion method in DCE and CS_2. The stoichiometries of CT complexes were determined by elemental analysis (C, H, N, S, halogen; the agreement between calculated and observed stoichiometry by elemental analysis is within 0.3%).

RESULTS AND DISCUSSION

Electron-Donating Property of HMTTeF

Table 1 compares the redox potentials, CT band energies of *s*-TNB complexes ($h\nu_{CT}$(*s*-TNB)) in solution of HMTTeF, HMTTF, HMTSF, and BEDT-TTF. For this comparison, we use DCE instead of AN for measuring cyclic voltammetry because the HMTTeF molecule is hardly soluble in AN.

The first oxidation potential ($E^{1}_{1/2}$(D)) of HMTTeF is between that of HMTTF and HMTSF. On the series of T*X*F (*X* = S, Se, Te) (1a) and DBT*X*F (*X* = S, Se, Te) (1b) molecules, the values of $E^{1}_{1/2}$(D) exhibit the same tendency.

The difference between the ionization potential of a donor and the electron affinity of an acceptor is essential for determining the ionicity, and thus conducting properties, of the CT complexes (10). Using photoelectron spectroscopy (PES) in the gas phase (11), both the first vertical and the adiabatic ionization potentials (I^{v}_{P}(D) and I^{ad}_{P}(D), respectively) are measured on HMTTF (6.41 and 6.06 eV, respectively), HMTSF (6.36 and 6.12 eV) and HMTTeF (7.22 eV and 6.81 eV) (12).

The $E^{1}_{1/2}$(D) is related to the adiabatic ionization potential. It has been known that the plot of I^{ad}_{P}(D) vs $E^{1}_{1/2}$(D) in AN for substituted TTF system donors shows a linear relation (11b):

$$I_{p^{ad}}(D) = eE_{1/2^1}(D)(\text{in AN}) + 5.76\ \text{eV}. \qquad [1]$$

On the other hand, the redox potential (E_{redox}) in DCE can be converted to that in AN by using an empirical relation between the E_{redox} values in AN and DCE for a number of acceptors and donors (13):

$$E_{redox}(\text{in DCE}) = 1.08\ E_{redox}(\text{in AN}) + 0.078. \qquad [2]$$

So, Eq. (1) is converted to Eq. (3) in DCE:

$$I_{P^{ad}}(D) = 0.93\ eE_{1/2^1}(D)(\text{in DCE}) + 5.69\ \text{eV}, \qquad [3]$$

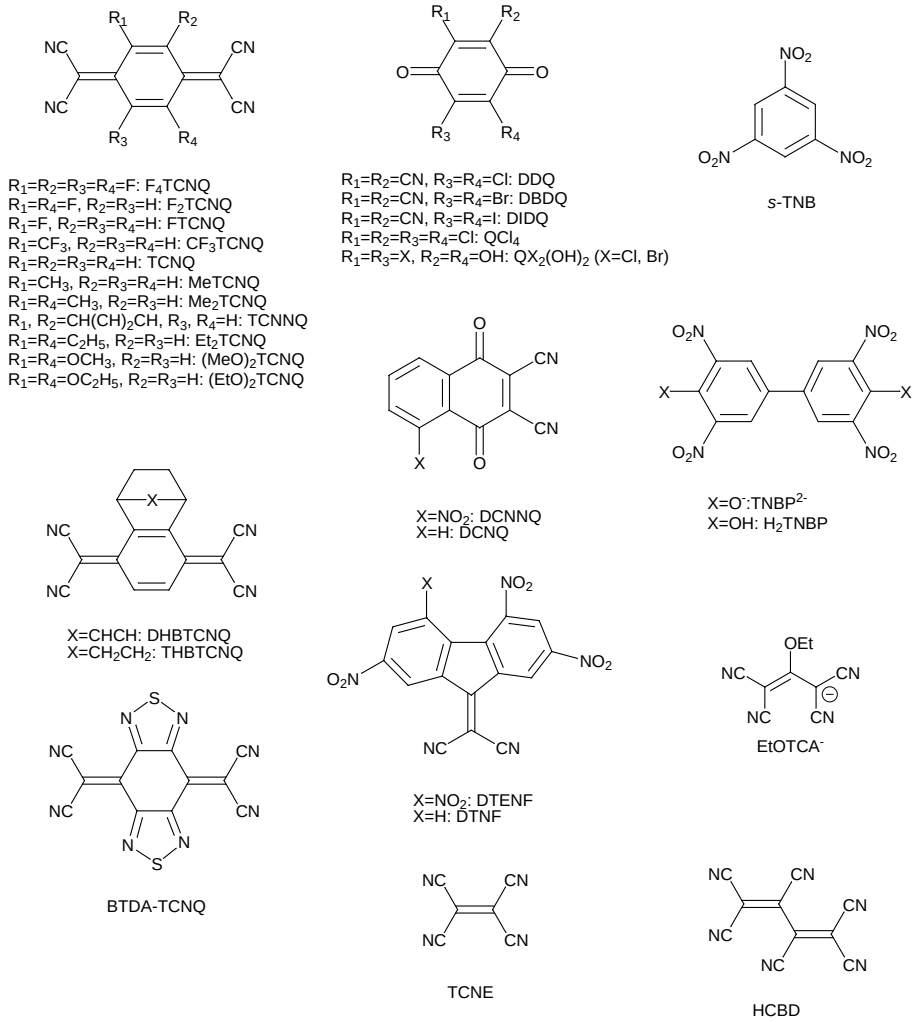

SCHEME 2. Acceptor molecules and organic anions used for preparation of HMTTeF complexes.

as shown in Fig. 1a. The $E^1_{1/2}$(D) values of HMTTF (b) and HMTSF (f), are nearly along the line of Eq. (1). However, HMTTeF shows a very large deviation from the linear relation, similar to TSF (g) and DBTTF (j). These deviations may be ascribed to their different solvation energies. On the plot of I^v_P(D) vs $h\nu_{CT}$(*s*-TNB), which is another approach for determining electron-donating ability of donor molecules (14), HMTTeF also resides far away from the linear relation. Since the plot of $E^1_{1/2}$(D) vs $h\nu_{CT}$ (*s*-TNB) (Fig. 1b) indicates a relatively good correspondence, $E^1_{1/2}$(D) or $h\nu_{CT}$(*s*-TNB) will be more appropriate parameters for measuring the donor strength including solvation energy.

TABLE 1

Redox Potentials ($E^1_{1/2}$(D) (V) vs SCE in DCE) and Charge Transfer Transition Energies of *s*-TNB Complexes in Solution ($h\nu_{CT}$(*s*-TNB)) of HMTT, HMTSF, HMTTeF, BEDO-TTF, and BEDT-TTF

Donor	Redox potentials		ΔE	$h\nu_{CT}(s-\text{TNB})$ ($10^3\,\text{cm}^{-1}$)
	$E^1_{1/2}$(D)	$E^2_{1/2}$(D)		
HMTTF	+0.42	+0.87	+0.45	13.7
HMTSF	+0.58	+0.96	+0.38	15.3
HMTTeF	+0.57	+0.87	+0.30	15.8
BEDO-TTF	+0.54	+0.89	+0.35	15.0
BEDT-TTF	+0.64	+0.97	+0.33	16.1

The difference (ΔE) between the $E^1_{1/2}$(D) and the second oxidation potential ($E^2_{1/2}$(D)) follows the trend HMTTF > HMTSF > HMTTeF, suggesting that the on-site Coulomb repulsion energy U decreases in this series.

Absorption Spectra in Solution

Neutral HMTTeF in solution exhibits strong absorption bands at 29.9×10^3 and 31.0×10^3 cm^{-1}, a weaker one at

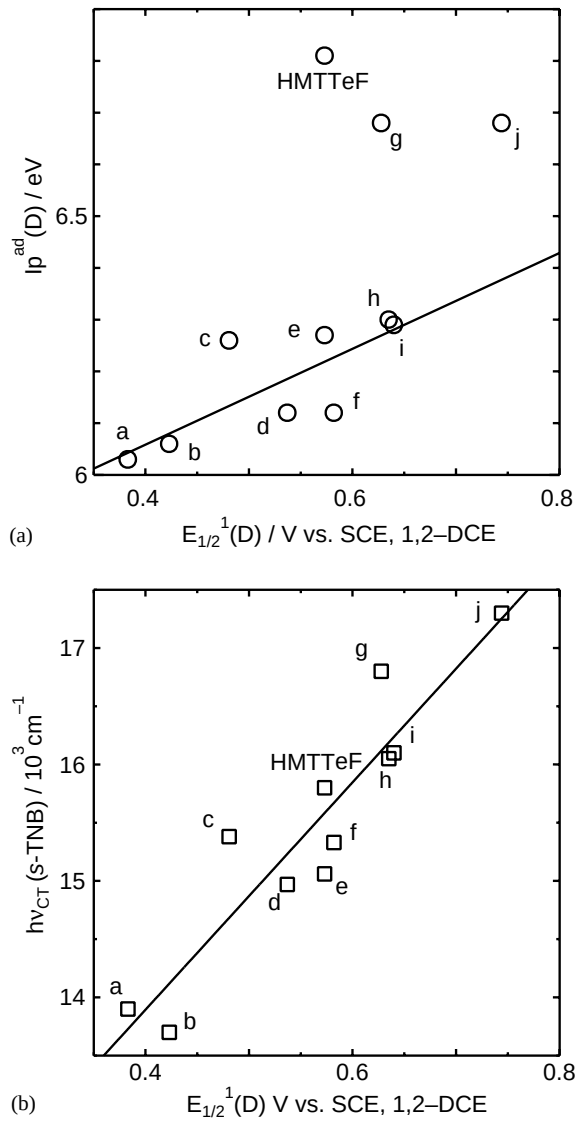

FIG. 1. (a) Correlation between the adiabatic ionization potential (I_p^{ad}(D)) and the first oxidation potential ($E_{1/2}^{1}$(D)) for (a) TMTTF, (b) HMTTF, (c) TTF, (d) BEDO-TTF, (e) TMTSF, (f) HMTSF, (g) TSF, (h) BEDT-TTF, (i) TTC_1-TTF and (j) DBTTF. The solid line represents Eq. (1). (b) Correlation between the charge transfer band energy (hv_{CT}(*s*-TNB)) and the first oxidation potential ($E_{1/2}^{1}$(D)) of the TTF derivatives used in (a). The solid line is a least-squares fit.

$24.1 \times 10^3\,cm^{-1}$ and much weaker HOMO-LUMO band at 15.9×10^3 (indicated by thin arrows on curve a in Fig. 2). While, the cation radical of HMTTeF (the $EtOTCA^-$ salt, $(HMTTeF)_2(EtOTCA)_2(PhCl)$ (15) in solution (curve b in Fig. 2) shows the lowest energy absorption (labeled band C) at $10.0 \times 10^3\,cm^{-1}$, a weak one at $15.5 \times 10^3\,cm^{-1}$ (band D), and rather strong one at $21.7 \times 10^3\,cm^{-1}$ (band E). An intense band at 30.1×10^3 cm^{-1} can be assigned to the intramolecular excitation of $EtOTCA^-$. The bands C, D and E in the solid spectrum (curve c in Fig. 2) of the $EtOTCA^-$ salt of HMTTeF are broadened and show a blue shift of about $1.5–2.0 \times 10^3$ cm^{-1} from those in solution. The lowest energy band at 7.9×10^3 cm^{-1} in the solid $EtOTCA^-$ salt is labeled band B. In the solution spectrum only the band B disappears, while others remain. Therefore, band B is associated with the optical transition between monocation radical molecules and is related to on-site Coulomb repulsion, U. This transition corresponds to the CT process, $D^+ + D^+ \rightarrow D^0 + D^{2+}$.

It is worth noting that the band B of the HMTTeF radical salt appears at a comparable position in the energy to those of the BEDT-TTF (BEDT-TTF · Br, 5.5×10^3 cm^{-1}) and BEDO-TTF (BEDO-TTF · I_3, $7 \sim 10 \times 10^3$ cm^{-1}) (16) salts but at considerably lower energy than those of HMTTF and HMTSF (17). This result confirms that the U value of the HMTTeF materials are relatively small, as was expected. The band C at around 11.0×10^3 cm^{-1}, which appears in the solid absorption spectrum of all HMTTeF CT complexes, is the lowest intramolecular transition and most likely originated from second HOMO to HOMO, as explained in other papers (14,18).

D–A-Type Complex Formation of HMTTeF

Because HMTTeF is a poor donor molecule, it is difficult to synthesize solid CT complexes, especially with weak acceptors. Good single crystals of HMTTeF complexes were obtained only with Et_2TCNQ and BTDA-

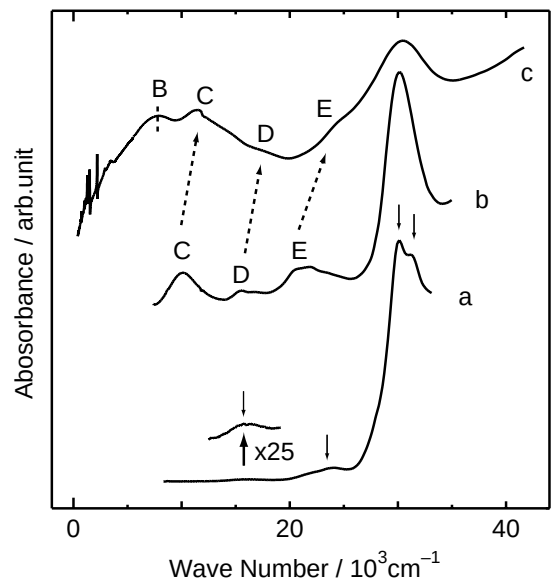

FIG. 2. Optical absorption spectra of (a) neutral HMTTeF in DCE solution, (b) $(HMTTeF)_2(EtOTCA)_2(PhCl)$ in DCE solution and (c) $(HMTTeF)_2(EtOTCA)_2(PhCl)$ on KBr pellet. See text for assignment of bands B–E. The absorption bands of neutral HMTTeF are indicated by arrows.

TCNQ. The characteristic properties of the D–A-type complexes of HMTTeF are summarized in Table 2. All HMTTeF complexes will be represented by their number of the first column in the table hereafter. The complexes are arranged according to the redox potentials of the acceptor molecules. It is noteworthy that the stoichiometry of several complexes is not simple. Namely, donor molecules are usually in excess and inclusion of solvent molecules occurs occasionally.

IR and UV-Vis-NIR Spectra

The CT band energy of the complexes with alternating stacking is related to the transition from $D^{+\gamma}A^{-\gamma}$ to $D^{+(1-\gamma)}A^{-(1-\gamma)}$, here γ is the CT degree, i.e. ionicity. The transition energies of the bands for neutral ($h\nu_{CT}^{N}$) and ionic complexes ($h\nu_{CT}^{I}$) are represented differently as

$$h\nu_{CT}^{N} = I_P(D) - E_A(A) - C' + X(\gamma < 0.5), \quad [4]$$

$$h\nu_{CT}^{I} = -I_P(D) + E_A(A) + (2\alpha - 1)C' + X'(\alpha > 0.5). \quad [5]$$

Here α is the Madelung constant, C' is the averaged electrostatic attraction energy of a D–A pair (defined as positive), and X, X' are mainly the resonance stabilization energies. So the neutral–ionic (N–I) phase boundary condition ($h\nu_{CT}^{N} = h\nu_{CT}^{I}$) gives

$$I_P(D) - E_A(A) = \alpha C' + (X' - X). \quad [6]$$

TABLE 2
Color, Shape, Stoichiometry, Optical, Conductivity, and Ionicity Data of HMTTeF Complexes Together with Redox Potentials ($E_{1/2}^{1}$(A) (V) vs SCE, in AN) of Acceptor Molecules

	Acceptor	$E_{1/2}^{1}$(A)	Stoichiometry (D : A : solvent[a])	Appearance	$h\nu_{CT}$ (10^3 cm^{-1})	σ_{RT} (Scm^{-1})	ε_a (meV)	I/P/N[b]
1	HCBD	+0.72	1 : 1	Black powder	3.0	9.1×10^{-2}	5.8×10	I or P
2	F_4TCNQ	+0.60	~1 : 1[c]	Blue powder	3.2	3.0×10^{-1}	3.4×10	I or P
3	DDQ	+0.56	1 : 1	Black powder	3.6	1.2×10^{-2}	4.6×10	I or P
4	DBDQ	+0.54	1 : 1	Black powder	5.9	2.0×10^{-3}	7.9×10	I or P
5	DIDQ	+0.51	1 : 0.95 : 0.5 (A)	Dark brown powder	5.9	5.0×10^{-4}	1.4×10^{2}	P
6	CF_3TCNQ	+0.44	4 : 3	Dark brown powder	4.9	4.1	3.2×10	P
7	F_2TCNQ	+0.41	1 : 0.9 : 0.4 (B)	Blue powder	3.4	2.9	4.5×10	P
8	DCNNQ	+0.38	1 : 0.75 : 0.4 (A) : 0.5 (B)	Black powder	4.9	3.5×10^{-3}	1.4×10^{2}	P
9	FTCNQ	+0.32	1 : 1	Blue powder	2.8	3.7×10^{-1}	1.0	P
10	TCNE	+0.29	1 : 1	Dull green powder	3.8	7.1×10^{-4}	6.9	P
11	DTENF	+0.23	3 : 2	Black powder	3.9	2.4×10^{-3}	8.0	P
12	TCNQ	+0.22	1 : 1	Dark green powder	2.9	7.1	3.0	P
13	DCNQ	+0.21	1 : 1	Brown powder	3.8	8.3×10^{-3}	7.1×10	P
14	MeTCNQ	+0.19	1 : 1	Black powder	2.6	1.8×10	1.0×10	P
15	DHBTCNQ	+0.18	1 : 0.5 : 0.2 (A)	Brown powder	3.1	7.6×10^{-4}	4.8×10	P
16	THBTCNQ	+0.16	1 : 0.6 : 0.3(A)	Brown powder	3.4	2.4×10^{-1}	6.2×10	P
17a	Et_2TCNQ	+0.15	1 : 1 : x (B, x = 0.5–1.0)	Black needle	5.1	1.0×10	Metallic–1.6×10[d]	P
17b	Et_2TCNQ	+0.15	2 : 1	Green powder	2.3	2.2	1.6×10–1.1×10^{2}	P
18a	Me_2TCNQ	+0.15	1 : 1 : 1(C)	Black needle	3.4	3.6×10	2.0–1.2×10	P
18b	Me_2TCNQ	+0.15	2 : 1	Green powder	2.7	4.5	2.4	P
19	TCNNQ	+0.07	1 : 1	Black powder	2.3	4.8	2.0×10	P
20	$(MeO)_2$TCNQ	+0.05	1 : 2	Blue powder	6.7	5.8×10^{-10}	3.0×10^{2}	N
21	QCl_4	+0.05	1 : 0.75 : 0.2(A)	Dark green powder	3.6	1.9	5.5×10	P
22a	BTDA-TCNQ	+0.03	1 : 1 : x(B, x = 0.5–1.0)	Black needle	5.0	4.2	2.1×10–4.9×10	P
22b	BTDA-TCNQ	+0.03	1 : 1	Black powder	2.6	8.3×10	3.0–8.3	P
23	DTNF	+0.02	1 : 1	Black powder	6.8	2.7×10^{-12}	5.0×10^{2}	N
24	$(EtO)_2$TCNQ	+0.01	1 : 1.2 : 0.1(A)	Brown powder	5.9	$<10^{-8}$	—	N
25	$QBr_2(OH)_2$	−0.12[e]	1 : 0.5 : 1(D)	Black powder	4.8	1.7	3.0×10	P
26	$QCl_2(OH)_2$	−0.13[e]	1 : 0.75 : 1(D)	Black powder	6.0	3.0×10^{-2}	3.6×10	P
27	C_{60}	−0.44[f]	1 : 1	Black rhombus crystal	1.2×10	$<10^{-8}$	—	N
28	TNBP	−0.55[e]	1 : 1	Brown powder	5.1	1.2×10^{-4}	1.8×10^{2}	P

[a] Solvents are represented by alphabets. A, PhCl; B, THF; C, DCE; and D, H_2O.
[b] Ionicities of the complexes are represented by: I, ionic; P, partial ionic; and N, neutral.
[c] See ref. (19).
[d] See ref (20).
[e] Peak potential.
[f] This value is converted from $E_{1/2}^{1}$(D) (in DCE) by Eq. (2).

Since the E_A(A) data are not available for many acceptors used, the ΔE(DA) ($=E^{l}_{1/2}$(D)$-E^{l}_{1/2}$(A)) value, which is originally related to the adiabatic values, I^{ad}_{P}(D) and E^{ad}_{A}(A) as previously described, is often used instead of the I_P(D)$-E_A$(A).

Figure 3 shows a plot of ΔE(DA) vs $h\nu_{CT}$ for all the DA-type complexes of HMTTeF. Equations (4) and (5) are depicted in the figure as a solid V-shaped line whose energy term of the right-hand side of Eq. (6) is taken as that for the TTF $\cdot$ *p*-quinone system as proposed by Torrance *et al.* (21). The dotted V-shape line is for the TCNQ system. This line shows a $+0.16$ V parallel shift from that of the solid V-shaped line due to the Mardelung energy difference from *p*-quinone system (18). This V-shaped diagram helps us to predict the ionicity and stacking manner of a CT complex (22).

The solid vertical lines in Fig. 3 represent

$$-0.02\text{V} \le \Delta E(\text{DA}) \le 0.34\text{V}. \qquad [7]$$

Equation (7) exhibits the partial ionicity regime of the 1 : 1 low-dimensional TTF $\cdot$ TCNQ system proposed by Saito and Ferraris (10b), according to the most simplified theory by McConnell *et al.* (23). The 1 : 1 CT complexes of the TTF $\cdot$ TCNQ system with a low-dimensional nature are fully ionic insulators in the region $\Delta E(\text{DA}) < -0.02$ V, whereas those in the region $\Delta E(\text{DA}) > 0.34$ V prefer an alternating stack and insulating state with a small γ (<0.5).

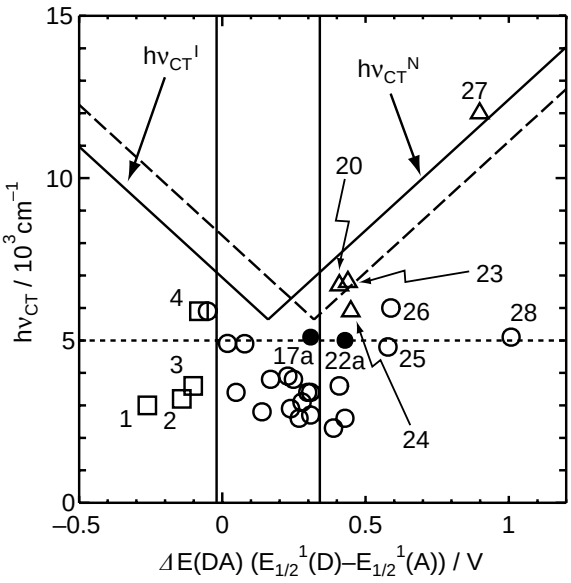

FIG. 3. Comparison of CT bands of HMTTeF complexes of D–A type in a KBr pellet ($h\nu_{CT}$) and ΔE(DA). Fully ionic (though partial CT state is not excluded for them, see text), partial CT and neutral complexes are represented by squares, circles and triangles, respectively. Equations (4) and (5) for TTF $\cdot$ *p*-quinone and TTFTCNQ system are represented by solid and dotted V-shape lines, respectively. The vertical lines represent Eq. (7). The numberings correspond to those listed in Table 2. Complexes **17a** and **22a** are depicted by filled circles.

Neutral Complex

Complexes **20**, **23**, **24** and **27** are classified as neutral CT complexes. This is in good agreement with the estimated ionicity based on Eq. [7]. Their vibrational spectra were approximated by the superposition of the neutral component materials. The first CT bands of these neutral complexes are scattered along the V-shaped line in Fig. 3.

Even though **28** may be classified as a neutral CT complex based on its donor and acceptor redox parameters its first CT band is located much lower, 5.1×10^3 cm^{-1}. Its IR spectrum exhibits not only superposition of neutral component materials but also those ascribable to the $TNBP^{2-}$, which is the dianion produced by losing protons from H_2TNBP. If all H_2TNBP molecules in **28** are deprotonated to $TNBP^{2-}$, its first CT band absorption should appear at around $7–8 \times 10^3$ cm^{-1}, similar to the case of the $EtOTCA^-$ salt. We suppose that some part of the H_2TNBP molecules in **28** is gradually deprotonated and changed to $TNBP^{2-}$ during its 1 month storage in the open air, similar to the complex preparation of $(TMTTF)_2(TNBP)$ (24). Its stoichiometry will be expressed by $(HMTTeF)(H_2TNBP)_{1-x}(TNBP^{2-})_x$, $x<0.5$. Its relatively low $h\nu_{CT}$ energy and good conductivity are consistent with the partial CT state of HMTTeF deduced from the formula.

The same features can be applied to the **25** and **26** complexes. Both exhibit low $h\nu_{CT}$ energies and good conductivities even though they should belong to the neutral complexes according to their redox parameters. They are composed of acceptor molecules containing the hydroxy groups, which presumably lose protons giving rise to mixed-valent anion species. In any case, HMTTeF molecules of **25**, **26** and **28** are classified into the partially ionized group because of their low-energy $h\nu_{CT}$ bands and good conductivities.

Ionic Complex

The fully ionic complexes afford sharp vibrational spectra which corresponds to the superposition of those of the ion radical component molecules (degree of CT is unity). Four complexes **1**, **2**, **3** and **4** all of which are 1 : 1 or nearly 1 : 1 stoichiometry are characterized to be fully ionic ($\gamma = 1$) based on their IR spectra. For example, most of the absorptions of the IR spectrum of **2** (Fig. 4) are composed of the ion radical component molecules ($EtOTCA^-$ salt and KF_4TCNQ, indicated by dotted lines). Although the fully ionic character of them is reasonably expected based on the redox properties of the component molecules, both the low CT energies and high conductivities are two of the

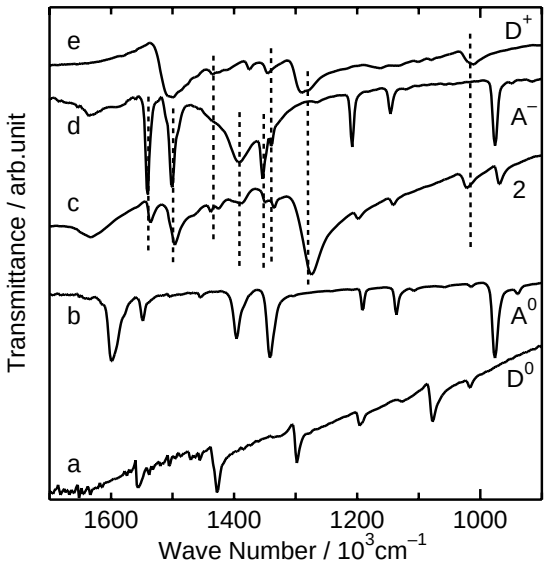

FIG. 4. IR spectra of (a) neutral HMTTeF (D^0), (b) neutral F_4TCNQ (A^0), (c) HMTTeF·F_4TCNQ (**2**), (d) KF_4TCNQ (A^-) and (e) (HMTTeF)$_2$(EtOTCA)$_2$(PhCl) (D^+) in a KBr pellet between 1700 and 900 cm^{-1}.

amazing features of the HMTTeF compounds since almost all nominally ionic CT complexes have been known to yield insulators except in a few very rare cases (25).

In Table 3, the electric conductivities and the first oxidation potentials of the donor molecules in several F_4TCNQ complexes are compared, where the donor strength of HMTTeF is medium among them. All of these F_4TCNQ complexes show complete charge transfer ($\gamma = 1$) and low conductivities except for the HMTTeF complex. In particular, even a weaker donor than HMTTeF yields a Mott insulator with F_4TCNQ; as seen with DBTTF and DBTSF which are the weakest donors in Table 3 (28,31). Therefore, F_4TCNQ is strong enough to ionize HMTTeF completely and all the reported results mentioned above predict that when the stoichiometry is 1 : 1 HMTTeF will produce an insulating complex with a complete CT, as long as the redox parameters are considered.

This prediction from the redox parameters seems to contradict the solid-state properties; not only the conductivity but also the electronic spectra (Fig. 5). Figure 5 compares the absorption bands of solid F_4TCNQ complexes with those of KF_4TCNQ. The absorption bands of the HMTTF, HMTSF and HMTTeF complexes of F_4TCNQ above 5×10^3 cm^{-1} are common among them and quite similar to those of the KF_4TCNQ in solid. These bands correspond to mainly the inter- (band B') and intramolecular (band C′ and E′) transitions of F_4TCNQ anion radical molecules. However, **2** indicates an extra absorption in the lower energy region (3.2×10^3 cm^{-1}). Consequently, it is concluded that the HMTTeF complex has a different electronic structure from the others, namely a partial CT state due to either: 1) the formation of a half-filled band with $\gamma = 1$ when $W > U$, (2) the formation of a partially filled band with $\gamma \neq 1$ even when $W < U$ or (3) a completely CT state ($\gamma = 1$) with small gap between valence and conduction bands, here W is the bandwidth.

TABLE 3

Conduction Properties of F_4TCNQ Complexes with Some TTF Derivatives. Donor Molecules Are Arranged According to the Redox Potentials ($E^1_{1/2}$(D) (V) vs SCE, in AN) of Donor Molecules. Alphabets of the First Column Are Represented in Fig. 1

Donor	$E^1_{1/2}$(D)	Degree of CT	Property/σ_{RT} (Scm^{-1})	Ref.
TMTTF (a)	+0.28		Insulator	32
HMTTF (b)	+0.29	1	1.0×10^{-4} (Mott insulator)	26
TTF (c)	+0.37	1	2.6×10^{-4} (dimerized)	30
TMTSF (e)	+0.45		Insulator	32
HMTTeF	+0.46[a]	1	3.0×10^{-1} ($\varepsilon_a = 3.4 \times 10$ meV, pellet)	This work
HMTSF (f)	+0.47	1	1.0×10^{-3} Mott insulator	27
BMDT-TTF	+0.52[a]	1	4.8×10^{-3}	29
BEDT-TTF(h)	+0.53	1	6.7×10^{-4}	29
BPDT-TTF	+0.53[a]	1	2.7×10^{-7}	29
DBTTF (j)	+0.63	1	Mott insulator	28
DBTSF	−[b]	1	Mott insulator	31

[a] These values are converted from $E^1_{1/2}$(D) (in DCE) by Eq. (2).
[b] Redox potential is not available.

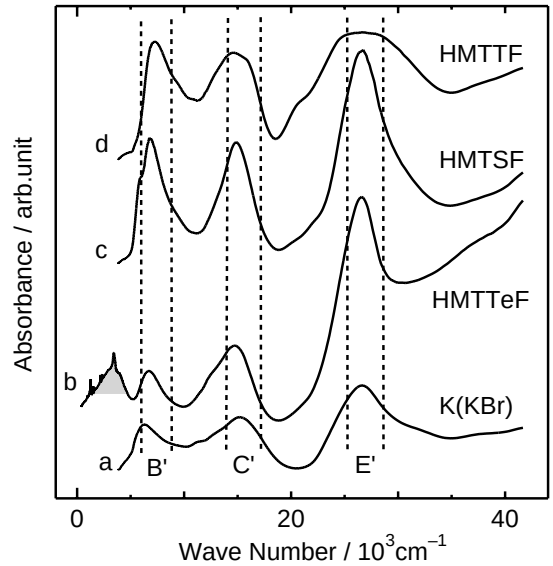

FIG. 5. UV–Vis–NIR spectrum of F_4TCNQ complex of (b) HMTTeF is compared with those of F_4TCNQ complexes of (c) HMTSF, (d) HMTTF and (a) K in a KBr pellet. See text for assignment of bands B′, C′ and E′.

The first one is eliminated since the compound has an activation energy for conduction ($3.4 \times 10-7.9 \times 10$ meV on a pellet samples of **1**–**4**). The results also preclude the partially filled band with $\gamma \neq 1$ in the second case. However, the second case with semiconductive nature due to non-uniform charge or stack is not eliminated. The second one is possible when the stoichiometry of the complex is not 1 : 1 but $1:n$ ($n<1$). Previously, the degree of CT of 0.75 was deduced from the C=C stretching frequency of the HMTTeF molecule by the Raman spectrum, 1391 cm^{-1}(33), while that of F_4TCNQ was estimated to be almost 1 for **2**, which had nearly 1 : 1 stoichiometry deduced by elemental analysis. The uncertainty in the estimation of the stoichiometry by elemental analysis allows 5% of deficiency of acceptor part even for the result of 1 : 1 based on the elements C, H, N and F for **2**. Therefore, it is possible that the complex is slightly out of stoichiometric ratio to give rise to a narrow gap semiconductor with partial CT in the HMTTeF part.

The last one is ascribed to the increased polarizability and decreased effective on-site Coulomb repulsion energy U_{eff} but also to the increased van der Waals radius of the chalcogenide atoms. The energy of a band B or B′ was approximated by.

$$h\nu_{CT}(\text{B-band}) \sim U_{\text{eff}}/2 + [U_{\text{eff}}^2/4 + 4t^2]^{1/2} - 2t. \quad [8]$$

In the case of the system of negligible transfer interactions t (such as the K salt of F_4TCNQ, curve a in Fig. 5), the band B appears at $(7–8) \times 10^3$ cm^{-1}. Such band B is also observed in the low conductive Mott insulator; the HMTTF or HMTSF salt of F_4TCNQ (curves c and d in Fig. 5) and in the conductive HMTTeF · F_4TCNQ (curve b in Fig. 5). As for the TTF derivatives B appears at around $(10–12) \times 10^3$ cm^{-1}. The polarizable nature of the component molecules effectively decreases U_{eff} and the band B appears at $(6–9) \times 10^3$ cm^{-1} in the 1 : 1 Br salts of BEDT-TTF or BEDO-TTF and the EtOTCA salt of HMTTeF (curve c in Fig. 2). It is highly expected that the increased van der Waals radius of Te enhances the intermolecular interactions between HMTTeF molecules more efficiently than the case of BEDT-TTF molecules giving rise to a relatively wide bandwidth of the HMTTeF complexes. Consequently, we have to include t in Eq. (8) and a band B may appear below 5×10^3 cm^{-1} as curve b in Fig. 5. In the assembly of a molecule with one electron, the HOMO band is split into upper Hubbard band and lower one by U_{eff} with a gap $\varepsilon_g = U_{\text{eff}}$. By introducing t, the gap is reduced by the bandwidth of the upper and lower HOMO bands and approximately gives

$$\varepsilon_g \sim (U_{\text{eff}}^2 + 16t^2)^{1/2} - 6t, \quad [9]$$

indicating that the gap is decreased with increasing t. Based on the energy gap for transport ($2\varepsilon_a$ = 68–116 meV for the HMTTeF complexes of **1**–**3**) and $h\nu_{CT}$(B-band) (370–450 meV for them), reasonable t and U_{eff} values are roughly estimated as 0.06–0.09 and 0.50–0.62 eV, respectively. Therefore, these complexes can be characterized as narrow gap semiconductor even in a fully ionic structure.

Partially Ionic Complex

All other 23 complexes in Table 2 have a characteristic low-energy band below 5.0×10^3 cm^{-1} (band A) and are highly conductive which is independent of the size and shape of the acceptor molecules. In Fig. 3 it is seen that they (○, ● in Fig. 3) are spread out over an extensive ΔE(DA) range, in particular in the neutral region compared to the one-dimensional organic metals, such as the 1 : 1 TTF-TCNQ system. This kind of feature has been observed in systems having a high electronic dimensionality of the segregated column or layer arising from the self-aggregation of the component molecules such as BEDO-TTF (14), bis(ethylenedioxy)-DBTTF (18) and ethylenedioxy-ethylenedithio-TTF (34). However, in the HMTTeF system the feature is not entirely ascribed to the self-assembling segregated stack as follows.

The electronic absorption spectra on the KBr pellet of the HMTTeF complexes are presented for some typical examples in Fig. 6. Every 1 : 1 partial CT complex whose acceptor belongs to the TCNQ system, such as **12** in Fig. 6, exhibits a band A together with a high σ_{RT} and small activation energy for conduction. In general, the appear-

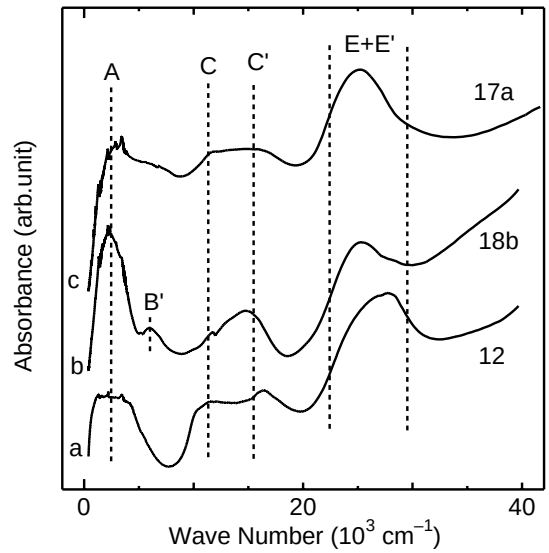

FIG. 6. UV–Vis–NIR spectra of (a) TCNQ (**12**), (b) Me_2TCNQ (**18b**), and (c) Et_2TCNQ (**17a**) complexes of HMTTeF in a KBr pellet. For the symbol of each band, see text and Figs. 2 and 5.

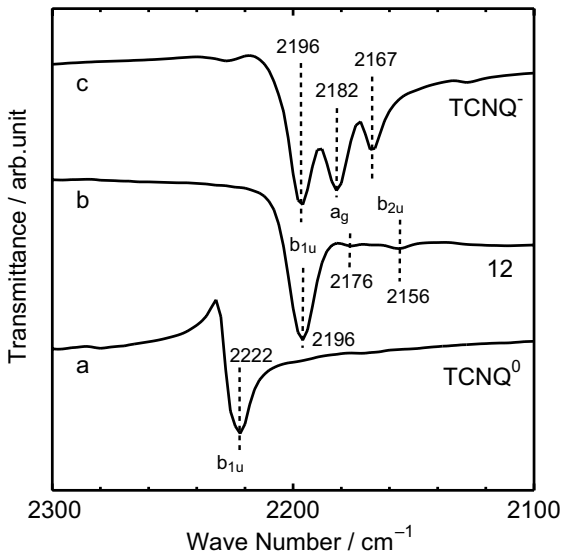

FIG. 7. Nitrile stretching modes (ν_{CN}) of (b) HMTTeF · TCNQ (**12**) are compared with those of (a) neutral TCNQ and (c) K · TCNQ in a KBr pellet.

ance of a band A indicates both a segregated column and a partial degree of CT including charge separation.

The IR spectrum of the TCNQ complex (**12**) is compared with those of neutral TCNQ and KTCNQ in Fig. 7 in the region of the CN stretching. Complex **12** exhibits no trace of bands ascribable to $TCNQ^0$ but one intense stretching mode (b_{1u}) at 2196 cm^{-1}, indicating no charge separation in the complex, and very faint kinks at 2176 (a_g mode) and 2156 cm^{-1} (b_{2u} mode). The very faint appearance of the a_g mode indicates that no distortion of the segregated column is present as far as the TCNQ molecule is concerned.

The highest frequency band ($b_{1u}\nu_{19}$) of the CN stretching bands of the TCNQ molecule is often used to estimate the charge on the TCNQ molecules in its CT complexes (28b). The estimated charge is $\gamma = 1$. However, this method for estimating the degree of CT is not very appropriate for highly ionized TCNQ complexes. Meanwhile, an empirical relationship between the degree of CT and the C–C wing stretching frequency in the Raman spectrum has been established for TCNQ complexes (35). The C–C stretching of 1403 cm^{-1} for the HMTTeFTCNQ has been observed yielding $\gamma = 0.64$ (33).

For the partial CT complexes containing excess donor molecules such as **18b** (2 : 1) in Fig. 6, γ values on the donor molecules can be deduced from both the stoichiometry and the precise assignment of the acceptor molecules. When the acceptor side is highly ionized and forms segregated assemblies, the absorption related to U of the acceptor molecule (band B') should appear in their electronic spectra. Complex **18b** is such a case and exhibits an absorption peak or shoulder assignable to band B' between 5 and 10×10^3 cm^{-1} as seen in Fig. 6, where γ of HMTTeF is deduced to be 0.5.

The 1 : 1 : x(THF) Et_2TCNQ (**17a**) and 1 : 1 : x(THF) BTDA-TCNQ (**22a**) complexes ($x = 0.5$–1.0) are exceptional cases. They reside around the bottom of the dashed V-shape line in Fig. 3 indicating that they are allocated around the N-I boundary. They exhibit a broad band A as shown by curve c in Fig. 6. Their IR spectra show the simultaneous coexistence of ionic and neutral species in the crystal. Structural analysis of them indicated that they have a uniform alternating stack of DA type (20). The band A is assignable to the CT transition between donor molecules along the perpendicular direction to the DA alternating stacking column, similar to those observed in the DA alternating BEDT-TTF complex of F_2TCNQ (36a) or ClMeTCNQ (36b), which exhibits a broad CT band around 4.3×10^3 cm^{-1}. Even though so far all complexes with a DA alternating stack were insulators, **17a** and **22a** exhibit a metallic nature near room temperature as shown below. This abnormal feature may have also occurred in many other 1 : 1 HMTTeF complexes of partial CT state including **12**.

Conductivity

Table 2 summarizes the room temperature conductivity (σ_{RT}) and the activation energy for conduction (ε_a). Most of the HMTTeF D–A-type complexes are obtained as powders, so the samples were measured in a compressed pellet form with the exception of **17a**, **18a**, **22a** and **27** which were measured as single crystals.

The neutral complexes (**20**, **23**, **24**, **27**) are insulating ($< 10^{-8}$ Scm^{-1}) in accordance with their high $h\nu_{CT}$ bands. On the other hand, the fully ionic complexes (though a partial CT state is not excluded) (**1**–**4**) exhibit relatively high σ_{RT} (3.0×10^{-1}–2.0×10^{-3} Scm^{-1}) and low ε_a (3.4×10–7.9×10 meV) as described above.

All the other partially ionic complexes exhibit highly conducting properties in general. Particularly, the partial CT complexes with a TCNQ system (**6**, **7**, **9**, **12**, **14**, **16**–**19**, **22**) are highly conductive except **15**. Their σ_{RT} are mainly more than 10^{-1} Scm^{-1} and ε_a less than 45 meV except **16**. It should be noted that the TCNQs in **15** and **16** are bulky ones. Though the *p*-quinone, percyano and fluorene systems have been known to be inferior for producing conductive CT complexes, HMTTeF yields conductive CT complexes (1.2×10^{-4}–1.9 Scm^{-1}).

The 1 : 1 : solvent complex of **17**, **18** or **22** yielded black single crystals of **17a**, **18a** or **22a**, respectively. The black powder **22b** has a stoichiometry of 1 : 1. On the other hand, the 2 : 1 modification of **17** or **18** is green powder (**17b** or **18b**). All of them are highly conductive. Complex **17a** has a $\sigma_{RT} = 30$ Scm^{-1} and exhibits a metallic behavior down to 230 K followed by a semiconducting behavior with

$\varepsilon_a = 1.6 \times 10$ meV (20). The ε_a of **17b**, **18a**, **22a** or **22b** is variable and gradually increases from room temperature down to lower temperatures, as shown in Table 2.

The single-crystal work of HMTTeF·TCNQ (1:1) indicates that at least this complex is metallic with a very high conductivity ($\sigma_{RT} = 1400\ Scm^{-1}$) (6). The compaction sample of this metallic complex shows $\sigma_{RT} = 7.1\ Scm^{-1}$ and $\varepsilon_a = 3.0$ meV, which is comparable to TTF·TCNQ, a typical organic metal, having $\sigma_{RT} = 30\ Scm^{-1}$ and $\varepsilon_a = 5.0$ meV in a compaction sample (37). These results suggest that **9**, **18a**, **18b** and **22b** may have a metallic nature if they are obtained as single crystals. Other CT complexes of HMTTeF which exhibit relatively good σ_{RT} and ε_a at room temperature above 5.0 meV can be regarded as narrow gap semiconductors.

Based on these conductivity results, it is clearly pointed out that tellurium atoms in the HMTTeF molecule have a peculiar ability to enhance the molecules to form the conductive columns or layers in the complex.

CONCLUSION

This work has demonstrated the peculiar ability of HMTTeF to produce a wide variety of conductive CT complexes of D–A-type independent of the size and shape of the acceptor molecules. This donor provides a few organic metals and a number of highly conductive powders. HMTTeF CT complexes with strong acceptor molecules, which are strong enough to ionize completely and generally afford insulators with the high $h\nu_{CT}$ energies that exhibit relatively high conductivities, small activation energy for conduction and low $h\nu_{CT}$ energies. In addition, the HMTTeF complex having a uniform alternating stack of DA type generally becomes an insulator exhibiting a metallic conduction with low $h\nu_{CT}$ energies. The intermolecular interactions are found to be strongly enhanced by both the bulky molecular orbital of HMTTeF and decreased on-site Coulomb repulsion in the HMTTeF complexes. These two factors especially seem to prevent both the fully ionic and the DA alternating HMTTeF complexes from becoming insulators, though the redox parameters and the crystal structures suggest them to be insulating.

ACKNOWLEDGMENTS

This work was in part supported by a Grant-in-Aid for Scientific Research from the Ministry of Education, Science, Sports, and Culture, Japan, a Grant for CREST (Core Research for Evolutional Science and Technology) of Japan Science and Technology Corporation (JST), a fund for "Research for Future" from Japan Society for Promotion of Science and a fund for the International Joint Research Grant Program of the New Energy and Industrial Technology Development Organization (NEDO).

REFERENCES

1. (a) R. D. McCullough, G. B. Kok, K. A. Lerstrup, and D. O. Kowan, *J. Am. Chem. Soc.* **109,** 4115 (1987); (b) K. Lerstrup, D. Talham, A. Bloch, T. Poehler, and D. O. Cowan, *J. Chem. Soc., Chem. Commun.* 336 (1982); (c) K. Lerstrup and D. O. Cowan, *J. Am. Chem. Soc.* **106,** 8303 (1984); (d) K. Lerstrup, A. Bailey, R. D. McCullough, M. Mays and D. O. Cowan, *Synth. Metals* **19,** 647 (1987); (e) D. J. Sandman, J. C, Stark and B. M. Foxman, *Organometallics* **1,** 741 (1982); (f) N. Okada, H. Yamochi, F. Shinozaki, K. Oshima and G. Saito, *Chem. Lett.* 1861 (1986); (g) M. R. Detty and B. J. Murry, *J. Org. Chem.* **47,** 1146 (1982).
2. G. Saito, T. Enoki, H. Inokuchi, H. Kumagai, and J. Tanaka, *Chem. Lett.* 503 (1983).
3. G. Saito, T. Enoki, K. Toriumi, and H. Inokuchi, *Solid State Commun.* **42,** 557 (1983).
4. F. Wudl and E. Ahron-Sharom, *J. Am. Chem. Soc.* **104,** 1154 (1982).
5. (a) K. Kikuchi, K. Yakushi, H. Kuroda, I. Ikemoto, K. Kobayashi, M. Honda, C. Katayama, and J. Tanaka, *Chem. Lett.* 419 (1985); (b) A. Kobayashi, Y. Sasaki, R. Kato, and H. Kobayashi, *Chem. Lett.* 387 (1986); (c) Z. S. Li, S. Matsuzaki, R. Kato, H. Kobayshi A. Kobayashi and M. Sano, *Chem. Lett.* 1105 (1986); (d) S. Matsuzaki, Z. S. Li and M. Sano, *Chem. Lett.* 1343 (1986); (e) S. Matsuzaki, Z. S. Li, and M. Sano, *Synth. Metals* **19,** 399 (1987); (f) D. O. Cowan, M. Mays, M. Lee, R. McCullough, A. Bailey, K. Lerstrup, F. Wiygul, T. Kistenmacher, T. Poehler, and L. Y. Chiang, *Mol. Cryst. Liq. Cryst.* **125,** 191 (1985).
6. G. Saito, H. Kumagai, J. Tanaka, T. Enoki, and H. Inokuchi, *Mol. Cryst. Liq. Cryst.* **120,** 337 (1985).
7. Abbreviations for chemicals in text: TTF, tetrathiafulvalene; TMTTF, tetramethyl-TTF; HMTTF, hexamethylene-TTF; DBTTF, dibenzo-TTF; TSF, tetraselenafulvalene; TMTSF, tetramethyl-TSF; HMTSF, hexamethylene-TSF; DBTSF, dibenzo-TSF; TTeF, tetratellurafulvalene; HMTTeF, hexamethylene-TTeF; DBTTeF, dibenzo-TTeF; BMDT-TTF, bis(methylenedithio)-TTF; BEDT-TTF; bis(ethylenedithio)-TTF; BPDT-TTF, bis(propylenedithio)-TTF; BEDO-TTF, bis(ethylenedioxy)-TTF; TTC_1-TTF, tetramethylthio-TTF; TCNQ, 7,7,8,8-tetracyano-*p*-quinodimethane; F_4TCNQ, tetrafluoro-TCNQ; CF_3TCNQ, trifluoromethyl-TCNQ; F_2TCNQ, 2,5-difluoro-TCNQ; FTCNQ, fluoro-TCNQ; MeTCNQ, methyl-TCNQ; Me_2TCNQ, 2,5-dimethyl-TCNQ; Et_2TCNQ, 2,5-diethyl-TCNQ; $(MeO)_2$TCNQ, 2,5-dimethoxy-TCNQ; $(EtO)_2$TCNQ, 2,5-diethoxy-TCNQ; BTDA-TCNQ, bis-1,2,5thiadiazolo-TCNQ; TCNNQ, tetracyanonaphtho-1,4-quinodimethane; DHBTCNQ, dihydrobarreleno-TCNQ; THBTCNQ, tetrahydrobarreleno-TCNQ; DDQ, 2,3-dichloro-5,6-dicyano-*p*-benzoquinone; DBDQ, 2,3-dibromo-5,6-dicyano-*p*-benzoquinone; DIDQ, 2,3-diiodo-5,6-dicyano-*p*-benzoquinone; QCl_4, 2,3,5,6-tetrachloro-*p*-benzoquinone; $QCl_2(OH)_2$, 2,5-dichloro-3,6-dihydroxy-*p*-benzoquinone; $QBr_2(OH)_2$, 2,5-dibromo-3,6-dihydroxy-*p*-benzoquinone; DCNQ, 2,3-dicyano-1,4-naphthoquinone, DCNNQ, 2,3-dicyano-5-nitro-1,4-naphthoquinone; DTENF, 9-(dicyanomethylene)-2,4,5,7-tetarnitrofluorene; DTNF, 9-(dicyanomethylene)-2,4,7-trinitrofluorene; H_2TNBP, 3,3′,5,5′-tetranitrobiphenyl-4,4'-diol; HCBD, hexacyano-1,3-butadiene; TCNE, tetracyanoethylene; *s*-TNB, sym-trinitrobenzene; $TNBP^{2-}$, 3,3',5,5'-tetranitrobiphenyl-4,4'-diol dianion; $EtOTCA^-$, 2-ethoxy-1,1,3,3-tetracyanoallyl anion; TBA^+, tetra(n-butyl)ammonium; AN, acetonitrile; DCE, 1,2-dichloroethane; PhCl, chlorobenzene; THF, tetrahydrofuran.
8. (a) N. Okada, G. Saito, and T. Mori, *Chem. Lett.* 311 (1986); (b) N. Okada, G. Saito, and T. Mori, *Synth. Metals* **19,** 589 (1987).
9. (a) O. W. Webster, *J. Chem. Soc.* **86,** 2898 (1964); (b) R. C. Wheland and E. L. Martin, *J. Org. Chem.* **40,** 3101 (1975); (c) J. Thiele and F. Günther, *Justus Liebigs Ann. Chem.* **349,** 45 (1906); (d) C. L. Jackson,

J. Am. Chem. Soc. **36,** 301 (1914); (e) H. Suzuki, A. Kondo, and T. Ogawa, *Chem. Lett.* 411 (1985); (f) M. Uno, K. Seto, M. Matsuda, W. Ueda, and S. Takahashi, *Tetrahedron Lett.* **26,** 1553 (1985); (g) K. Wallenfells, G. Backman, D. Hofmann, and R. Kern, *Tetrahedron* **21,** 2239 (1965); (h) O. Hutzinger, R. A. Haecock, J. D. Macneil, and R. W. Frei, *J. Chromatogr.* **68,** 173 (1972); (i) G. A. Reynolds and J. A. Vanallen, *J. Org. Chem.* **29,** 3591 (1964); (j) Y. Yamashita, T. Suzuki, T. Mukai, and G. Saito *J. Chem. Soc., Chem. Commun.* 1044 (1985); (k) T. K. Mukherjee and L. A. Levasseuer, *J. Org. Chem.* **30,** 644 (1965); (l) E. Kunze, *Chem. Ber.* **21,** 3331 (1888).

10. (a) J. B. Torrance, *Acc. Chem. Res.* **12,** 79 (1979); (b) G. Saito and J. P. Ferraris, *Bull. Chem. Soc. Jpn.* **53,** 2141 (1980).
11. (a) D. L. Lichtenberger, R. L. Johnston, K. Hinkelmann, T. Suzuki, and F. Wudl, *J. Am. Chem. Soc.* **112,** 3302 (1990); (b) N. Sato, G. Saito, and H. Inokuchi, *Chem. Phys.* **76,** 79 (1983) and references cited therein.
12. N. Sato, G. Saito, and H. Inokuchi, *Chem. Phys.* **126,** 395 (1988).
13. G. Saito, T. Teramoto, A. Otsuka, Y. Sugita, T. Ban, M. Kusunoki, and K. Sakaguchi, *Synth. Metals* **64,** 359 (1994).
14. S. Horiuchi, H. Yamochi, G. Saito, K. Sakaguchi, and M. Kusunoki, *J. Am. Chem. Soc.* **118,** 8604 (1996).
15. S. S. Pac and G. Saito, *Synth. Metals* **102,** 1705 (1999).
16. S. Horiuchi, H. Yamochi, G. Saito, and K. Matsumoto, *Mol. Cryst. Liq. Cryst.* **284,** 357 (1996).
17. Band B of cation radical salt of HMTTF or HMTSF related to effective *U* value is not reported. It may be not much different from that of TMTTF or TMTSF; 10×10^3 cm^{-1}.
18. T. Senga, K. Kamoshida, L. A. Kushch, G. Saito, T. Inayoshi, and I. Ono, *Mol. Cryst. Liq. Cryst.* **296,** 97 (1997).
19. The elemental analysis for **2** (C, H, N and F) is tried at several times, and the stoichimetry of **2** is in the rage of 1:0.95 and 1:1:0.35(PhCl).
20. G. Saito, S. S. Pac, and O. O. Drozdova, *Synth. Metals* **120,** 667 (2001).
21. (a) R. Foster, "Organic Charge Transfer Complexes." Academic Press, London, 1969; (b) J. B. Torrance, J. E. Vaquenz, J. J. Mayerle, and V. Y. Lee, *Phys. Rev. Lett.* **46,** 253 (1981).
22. (a) K. Nakasuji, *Pure Appl. Chem.* **62,** 477 (1990); (b) Strictly speaking, the stacking manner is not determined solely from the analysis for the diagram of Fig. 3, although such exceptions are few. For example, some fully ionic complexes with alternating stacking show the absorption of CT process among D^+ (or A^-) molecules instead of the back CT absorption (from A^- to D^+). Also, few weak neutral complexes of bezidines and 4,4'-dinitrobiphenyl show a transition from D^0 to A^0, however, the complexes have a kind of segregated stacking manner; K. Abe, Y. Matsunaga, and G. Saito, *Bull. Chem. Soc. Jpn.* **41,** 2852 (1968).
23. H. M. McConnell, B. M. Hoffman, and R. M. Metzger, *Proc. Natl. Acad. Sci. USA* **53,** 46 (1965).
24. K. Nishimura, G. Saito, G. G. Abashev, and A. G. Tenishev, *Synth. Metals* **120,** 911 (2001).
25. (a) Y. Misaki, H. Nishikawa, K. Kawkami, S. Koyanagi, T. Yamabe and M. Shiro, *Chem. Lett.* 2321 (1992); (b) Y. Misaki, H. Nishikawa, K. Kawkami, S. Koyanagi, T. Yamabe, and M. Shiro, *Bull. Chem. Soc. Jpn.* **67,** 661 (1994); (c) T. Mori, H. Inokuchi, Y. Misaki, T. Yamabe, H. Mori and S. Tanaka, *Bull. Chem. Soc. Jpn.* **67,** 661 (1994); (d) K. Takiyama, A. Ohnishi, Y. Aso, T. Otsubo, F. Ogura, K. Kawabata, K. Tanaka, and M. Mizutani, *Bull. Chem. Soc. Jpn.* **67,** 766 (1994).
26. (a) J. B. Torrance, J. J. Mayerle, K. Bechgaard, B .D. Silverman, and Y. Tomkiewicz, *Phys. Rev. B.* **22,** 4960 (1980); (b) J. B. Torrance, J. J. Mayerle, K. Bechgaard, B .D. Silverman and Y. Tomkiewicz, *Phys. Rev. B.* **26,** 2267 (1982).
27. (a) M. E. Hawley, T. O. Poehler, T. F. Carruth, A. N. Bloch, D. O. Cowan, and T. J. Kistenmacher, *Bull. Am. Phys. Soc.* **23,** 424 (1978); (b) J. P. Stokes, A. N. Bloch, W. A. Bryden, D. O. Cowan, M. E. Hawley and T. O. Poehler, *Bull. Am. Phys. Soc.* **24,** 232 (1979).
28. (a) T. J. Emge, W. A. Bryden, F. M. Wiygul, D. O. Cowan, and A. N. Bloch, *J. Chem. Phys.* **77,** 3188 (1982); (b) J. S. Chappel, A. N. Bloch, W. A. Bryden, M. Maxfield, T. O. Poehler, and D. O. Cowan, *J. Am. Chem. Soc.* **103,** 2422 (1981).
29. G. Saito, H. Hayashi, T. Enoki, and H. Inokushi, *Mol. Cryst. Liq. Cryst.* **120,** 341 (1985).
30. (a) R. C. Wheland and J. L. Gillson, *J. Am. Chem. Soc.* **77,** 3188 (1976); (b) F. M. Wiygul, *Mol. Cryst. Liq. Cryst.* **22,** 4760 (1980).
31. K. Lerstrup, M. Lee, F. W. Wiygul, T. J. Kistenmacher, and A. N. Bloch, *J. Chem. Soc., Chem. Commun.* 294 (1983).
32. G. Saito, unpublished results.
33. Z. S. Li, S. Matsuzaki, M. Onomichi, M. Sano, and G. Saito, *Synth. Metals.* **16,** 71 (1986).
34. G. Saito, H. Sasaki, T. Aoki, Y. Yoshida, A. Otsuka, H. Yamochi, O. O. Drozdova, K. Yakushi, H. Kitagawa, and T. Mitani, *J. Mater. Chem.* **12,** 1640 (2002).
35. (a) S. Matsuzaki, R. Kuwata, and K. Toyoda, *Solid State Commun.* **33,** 403 (1980); (b) S. Matsuzaki, T. Moriyama, and K. Toyoda, *Solid State Commun.* **34,** 857 (1980).
36. (a) T. Hasegawa, S. Kagoshima, T. Mochida, S. Sugiura, and Y. Iwasa, *Solid State Commun.* **103**(8), 489 (1997); (b) T. Hasegawa, T. Mochida, R. Kondo, S. Kagoshima, Y. Iwasa, T. Akutagawa, T. Nakamura, and G. Saito, *Phys. Rev. B* **62**(15), 10 059 (2000).
37. L. B. Coleman, *Rev. Sci. Instrum.* **49**(1), 58 (1978).